Genetics in Medicine Open (2024) 2, 101884

ELSEVIER

Genetics in Medicine OPEN
An Official Journal of the ACMG

www.journals.elsevier.com/genetics-in-medicine-open

ARTICLE

Automated fingerprint analysis as a diagnostic tool for the genetic disorder Kabuki syndrome

Viktor Ingi Agustsson[1,2], Pall Asgeir Bjornsson[3], Ashildur Fridriksdottir[3], Hans Tomas Bjornsson[1,2,4,5,*], Lotta Maria Ellingsen[3,*]

[1]*Faculty of Medicine, University of Iceland, Reykjavik, Iceland;* [2]*Department of Genetics and Molecular Medicine, Landspitali University Hospital, Reykjavik, Iceland;* [3]*Faculty of Electrical and Computer Engineering, University of Iceland, Reykjavik, Iceland;* [4]*Louma G. Laboratory of Epigenetic Research, Faculty of Medicine, University of Iceland, Reykjavik, Iceland;* [5]*McKusick-Nathans Department of Genetic Medicine, Johns Hopkins University School of Medicine, Baltimore, MD*

ARTICLE INFO

Article history:
Received 9 February 2024
Received in revised form
25 July 2024
Accepted 28 July 2024
Available online 7 August 2024

Keywords:
Artificial intelligence
Artificial neural network
Dermatoglyphics
Digital diagnostics
Fetal fingertip pads

ABSTRACT

Purpose: Emerging therapeutic strategies for Kabuki syndrome (KS) make early diagnosis critical. Fingerprint analysis as a diagnostic aid for KS diagnosis could facilitate early diagnosis and expand the current patient base for clinical trials and natural history studies.
Method: Fingerprints of 74 individuals with KS, 1 individual with a KS-like phenotype, and 108 controls were collected through a mobile app. KS fingerprint patterns were studied using logistic regression and a convolutional neural network to differentiate KS individuals from controls.
Results: Our analysis identified 2 novel KS metrics (folding finger ridge count and simple pattern), which significantly differentiated KS fingerprints from controls, producing an area under the receiver operating characteristic curve value of 0.82 [0.75; 0.89] and a likelihood ratio of 9.0. This metric showed a sensitivity of 35.6% [23.73%; 47.46%] and a specificity of 96.04% [92.08%; 99.01%]. An independent artificial intelligence convolutional neural network classification-based method validated this finding and yielded comparable results, with a likelihood ratio of 8.7, sensitivity of 76.6%, and specificity of 91.2%.
Conclusion: Our findings suggest that automatic fingerprint analysis can have diagnostic use for KS and possible future utility for diagnosing other genetic disorders, enabling greater access to genetic diagnosis in areas with limited availability of genetic testing.

Introduction

The hypothesis that abnormal dermatoglyphics are connected to early disruption of fetal development dates back to the 1950s when noticeable pattern differences were reported between individuals with Down syndrome and healthy controls.[1] Substantial literature exists linking genetic variation and abnormal dermatoglyphics, and in the era of limited

The Article Publishing Charge (APC) for this article was paid by Hans Tomas Bjornsson.
*Correspondence and requests for materials should be addressed to Hans Tomas Bjornsson, Faculty of Medicine, University of Iceland, Vatnsmyrarvegur 16, 101 Reykjavik, Iceland. *Email address:* htb@hi.is OR Lotta Maria Ellingsen, Faculty of Electrical and Computer Engineering, University of Iceland, Dunhagi 5, 107 Reykjavik, Iceland. *Email address:* lotta@hi.is

doi: https://doi.org/10.1016/j.gimo.2024.101884

availability of genetic diagnosis, there was considerable interest in using distinct fingerprint patterns to aid in the diagnosis of genetic disease.[1-4] The fingerprint patterns themselves are known to be a highly heritable trait,[5] thought to be greatly affected by neonatal topographical alteration of the dermal surface, as well as genetic variation of limb developmental genes.[6,7] The pattern appears particularly dependent on the process of volar pad regression in the first weeks of life, which helps determine the pattern of dermal folding (Supplemental Figure 1A-C).[8] The dwindling interest in dermatoglyphics as a diagnostic tool, after the wide availability of genetic testing in resource-abundant societies, has left the area largely unexplored, in particular, in relation to recent advancements in automatic digital image processing and artificial intelligence. However, in the interest of providing wider access to genetic testing to disadvantaged populations of the world,[9-11] an inexpensive and noninvasive diagnostic tool could be a useful tool in combination with currently available tools such as Face2Gene[12] and clinical diagnostic criteria.[13] This would help prioritize which individuals should get genetic testing, thereby reducing cost and reliance on dysmorphological expertise.

Kabuki syndrome (KS), commonly caused by heterozygous de novo variants in either *KMT2D* (KS1, OMIM: #147920) or *KDM6A* (KS2, OMIM: #300867),[13] offers a promising disorder to examine the usefulness of using dermatoglyphic abnormalities combined with artificial intelligence as a diagnostic tool to aid in genetic diagnosis. Dermatoglyphic abnormalities have been documented since the time of KS description by Niikawa et al,[14,15] in which researchers reported increased frequency of digital ulnar loops and absence of digital triradius C and/or D, and one of its key characteristics was the presence of persistent fetal fingertip pads, thought to arise from abnormal volar pad regression during fetal development (Supplemental Figure 1A-D).[13,15] If one was able to utilize image analysis of individual fingerprints to test whether these known dermatoglyphic abnormalities or other unknown abnormalities could aid in the diagnosis of KS, a disorder in which preclinical work has been promising, this would help establish the true prevalence of the disorder.[16-18] Furthermore, clinical trials would benefit from patients being diagnosed at an earlier time point and from expanding the pool of eligible participants. This would shorten the diagnostic journey for individuals living in regions where there is limited availability of genetic testing because of paucity of genetics expertise.

The implementation of artificial intelligence is expected to revolutionize medicine by incorporating complex data with increased computational power to improve clinical outcome.[19] Deep neural networks (DNNs), a subcategory of artificial intelligence, have opened up novel possibilities to resolve complex and specialized analytical problems unachievable by previous computational methods through neuronal-like decision models, in which processing nodes simulate inter-neurons of the central nervous system. Recent examples include the AlphaFold Protein Structure Database, in which 3D protein structure predictions are provided to the scientific community using linear amino acid sequence as the models input.[20] By using predicted protein structures a new program called AlphaMissense (https://github.com/google-deepmind/alphamissense), is used to predict pathogenicity of missense variants.[21] In addition, deep neural networks are being used as a diagnostic aid for syndromes with known facial dysmorphic features by using facial image analysis. An example of this is DeepGestalt (the neural network behind Face2Gene), which was trained on images from over 200 syndromes from a community-driven phenotype platform to extract facial features for rare syndrome diagnosis. The neural network produces a diagnostic score for different genetic syndromes.[12] Marwah et al[22] report that the correct diagnosis is seen as one of the top-10 most likely diagnosis in 90% of instances. Point-of-care assessment showed that in an undiagnosed population, which includes syndromes that DeepGestalt was not trained on, that number was 57%. DNNs are starting to extend into the clinic, where, for example, image-based pathological identification has been shown to be successful as a screening tool.[23-26]

Here, we have systematically examined the dermatoglyphic abnormalities in fingerprint images of individuals with KS and assessed their clinical value in the form of a case-control study using 2 independent classification strategies: a machine learning approach using a novel metric of fingerprint patterns as an input, and a DNN strategy using fingerprint images as an input.

Specialized pattern metrics support that convolutional neural networks (CNNs) can be used to successfully identify KS individuals from unaffected individuals. This proof-of-principle study for KS can in the future be expanded to other genetic disorders and indicates, in theory, that 1 or more genetic disorder can be directly diagnosed with a fingerprint scanner from an individual's smartphone in the not-too-distant future.

Materials and Methods

Recruitment of the clinical cohort

Participants were recruited through 2 clinical sites (Landspitali University Hospital, Reykjavik, Iceland, and Johns Hopkins Hospital, Baltimore, USA) and 3 individual patient organized conferences (United Kingdom, Seattle, and Texas). Recruitment occurred in the period ranging from June 2020 until December 2022. Information about genetic variants (when available) was documented along with potential confounders, such as age, sex, and ethnicity (self-reported). The case group consisted of individuals with self-reported KS. All patients except 13 had a known disease-causing variant and could self-report whether *KMT2D* or *KDM6A* variants had been found, although only 30 individuals were able to provide detailed formal genetic report to share with the investigators. Eight of these 13 individuals without reported disease-causing variant knew that

it was either *KMT2D* or *KDM6A*, and the remaining 5 had a clinical diagnosis of KS.

The control group consisted of either family members of KS individuals, which are assumed to be unaffected because KS is almost exclusively caused by de novo changes or alternatively, individuals who sought genetic counseling because of a suspected genetic abnormality unrelated to KS. The effect of a possible genetic abnormality was documented along with information about results of genetic testing or clinical diagnosis. One participant, an individual with Kabuki-like syndrome (Turner syndrome with a ring X chromosome), was documented separately. Informed consent for individuals with KS and family members was obtained for all 108 controls and 75 cases using Institutional Review Board approved protocols from either the Johns Hopkins Hospital (NA_00079185) or from the ethical board of Landspitali University Hospital (VRN_211118) and the National Bioethics Committee (VSN_21-228).

The GenePrint app

A specialized smartphone app, named GenePrint, was developed for the collection of the data required for this study, including fingerprint images, demographic information, and genetic variant information. The app was developed and implemented using Java and SQLite. Currently, the app requires an external optical fingerprint scanner to be connected to the smartphone. The app guides the data collector through the collection process using a visual graphical representation of each scanned finger and its relative location. The app stores data for each participant separately on the smartphone, and anonymized data can then be submitted to a secure database. GenePrint currently supports Android 4.4-11.0 and can be downloaded through APKFab (https://apkfab.com/).

Image collection

Fingerprint image collection was performed using HID DigitalPersona 4500 Fingerprint Reader (HID Global) connected to a smartphone with the GenePrint app installed. To make data collection more consistent between different data collectors, we developed our own standardized protocol for the fingerprint collection (see Supplemental Appendix 1 and 2). Fingerprints were collected individually from each of the 10 fingers of each participant. For 2 KS participants, fingerprints were collected at 2 times for each finger within a 2-year interval for improved image quality. Only 1 data collection (10 fingerprints) was used for each participant in the fingerprint analysis described below.

Image Conversion, enhancement, and variable identification

The raw fingerprint images were converted to 8-bit RGB PNG images using Python. An enhancement algorithm was used for noise reduction because of impression conditions. The algorithm is based on the convolution of normalized images with a series of Gabor filters tuned to the local ridge orientation and frequency in addition to pixel binarization (see Supplemental Figure 2) (Bansal R, Sehgal P, Bedi P. Minutiae extraction from fingerprint images – a review. arXiv preprint arXiv:1201.1422. https://doi.org/10.48550/arXiv.1201.1422). The image enhancement method is available as open source on Github.[27] The ridge enhanced images were used for variable extraction and CNN classification.

Components of fingerprint patterns were visually and/or automatically assessed using R and Python. Quality measurements for each fingerprint were documented through a binary marker of core visibility (excluding arch type patterns) and quality score from the fingerprint identification software NIST Fingerprint Image Quality 2 (NFIQ 2) from the National Institute of Standards and Technology (NIST).[28] The NFIQ2 score is a quality score, which quantifies the quality and quantity of fingerprint patterns that are used for fingerprint identification. The numerical values range from 0, which is the worst quality score, to 100, which is the best quality score. Folding finger ridge (FFR), a horizontal line through the fingerprint direction, (see Supplemental Figure 2), was visually documented in a randomized blinded fashion with multiple sets of images, each set containing approximately 250 images of equal group distribution, along with assigned Henry's fingerprint classification.[29] Henry's classification categorizes dermatoglyphic patterns into 3 groups (arch, loops, and whorls), which can be further subdivided into 8 subgroups (tented arch, plain arch, ulnar loop, radial loop, simple whorl, central pocketed whorl, double loop whorl, and accidental whorl).[29] An additional quality check was performed for Henry's classification by comparing patterns of each individual's opposite fingers for classification discrepancy. If visual inspection confirmed pattern discrepancies between opposite fingers, then the fingerprint images were marked for reclassification and added to the next documentation patch. The discrepancy check was performed because a symmetrical pattern was quite common for opposite fingers of the same participant.

The FFR count (FFRC), which is the count of intersected fingerprint ridge lines to a vertical line stretching to the FFR from the pattern core, was computed by an automatic counting algorithm on ridge enhanced and skeletonized images. Visual confirmation of the correct location of the intersections was needed to validate the FFRC value. In cases in which the automatic counting failed, visual counting determined the FFRC value. Apparent gross misalignment of a fingerprint to the direction of the digital fingerprint scanner at the time of fingerprint collection, using 30 degrees as a reference for gross misalignment to avoid correcting for mild clinodactyly, was corrected through visual assessment of the vertical line in the direction of the finger. FFRC was documented in a blinded way as was done for the FFR. The FFRC evaluation processes is demonstrated in Supplemental Figure 2, and the counting code is available through GitHub (https://github.com/ViktorIngi/Fingerprint-

ridge-count). Ridge enhancement and skeletonization were performed using an open access software available on Github.[27,30]

Single variable analysis

Preliminary analysis was conducted with $n = 11$ KS and $n = 53$ control subjects, comparing different pattern characteristics to identify key variables for separating KS from controls. The 2 most prominent variables, participant's mean FFRC (mFFRC) and lack of individual pattern variability, were further evaluated with a larger sample size of $n = 43$ for the KS group and $n = 70$ for the control group. Individual pattern variability was defined as individual-based proportion of the combined amount of simple whorl and ulnar loop. At the time of reevaluation, the lack of individual pattern variability was redefined to proportional maximum of 1 of the 8 Henry's patterns (the variable will be hereafter referred to as the "simple pattern"). Calculations of proportions were in both cases isolated to classifiable patterns by Henry's classification and limited to 8 or more fingerprints. Redefinition was performed for the purpose of a more descriptive variable for the lack of individual's pattern variability. For group comparison, Welch Two Sample t test was used for mFFRC and Fisher's exact test was used for the lack of individual pattern variability and simple pattern, with values ≥ 0.8 and ≥ 0.9 marked as a positive outcome, respectively. Despite insignificant preliminary findings of ulnar loops frequency, the variable was reevaluated on the complete dataset of adequate quality for Henry's classification because increased ulnar loops was one of the features described at the time of KS discovery.[14]

The additional variable of ridge density (Supplemental Figure 3), a value of counted ridge intersections with two 100 pixel spanning lines with either +45 degrees or −45 degrees angle to a line spanning from the fingerprint core upward and adjacent to the fingerprint direction, was evaluated. Ridge counting code, similar to the one for FFRC, was used to determine the density values (code available through GitHub, https://github.com/ViktorIngi/Fingerprint-ridge-count) with identical preprocessing of the images as was used for the FFRC. Mean density values were obtained for $n = 94$ controls and $n = 59$ KS participants where participants with 2 or fewer ridge density values were excluded, and Wilcoxon test was used for age-dependent comparison.

Logistic regression classification

The 2 variables, mFFRC and simple pattern, were used for logistic regression modeling. The ulnar loop was excluded from the model because of its inferior performance compared with the simple pattern when variables were interchanged (simultaneous use risks multicollinearity). The case group consisted of KS participants and the Kabuki-like participant, given the clinical overlap and mFFRC value similarity to the KS group. Participants with 7 or less Henry's classifiable fingerprints were excluded from the models, mirroring the data exclusion for simple patterns and mFFRC. Participants without mFFRC value were assigned a value of 1.5 times the group maximum of mFFRC by the rationale that the distance of the FFR was most likely too far from the core to be scannable (or simply not present) and the assignment of greater distance would encrypt the FFR absence.

Two logistic regression models were trained. Training of the primary model used leave-one-out cross validation (LOOCV) of $n = 64$ controls and $n = 32$ cases. The primary model was then tested by using unseen data, $n = 37$ controls and $n = 27$ cases, collected after primary modeling. The secondary model was identical to the primary model except that it included all the unseen data as well, a total of $n = 101$ controls and $n = 59$ cases for the training. LOOCV was used to determine the primary and secondary model performance. The package pROC was used for sensitivity, specificity, and area under the receiver operating characteristic curve (AUC) calculations,[31] and the package Classification and Regression Training (caret)[32] was used for the regression models. Sensitivity is the proportion of correctly identified individuals with KS. In contrast, specificity is the proportion of non-KS individuals identified correctly by our test.

CNN classification

A CNN model was implemented and trained on individual fingerprint images for case vs control classification, either unaltered or ridge enhanced (as described above). Different quality measurements were used to exclude data of poor quality (see details in the Results Section). Before training, 10% of the data were left out as unseen (held-out) testing data. The remaining data were used for CNN model training, in which 5-fold cross validation was utilized (with each fold split into 80% as training and 20% as test data). The average outcome of the model accuracy, sensitivity, and specificity was calculated from each validation fold from the 5-fold cross validation along with the 95% confidence interval (CI) from the standard deviation. Fingerprint predictions in each fold were marked and evaluated for 5-fold cross validation performance, in relation to sampling location. The performance of the CNN model was evaluated on the unseen test data in a similar way without the possibility of calculating CI.

CNN hyperparameter selection and regularization

Our model was trained using dual Nvidia GeForce RTX 2080 Ti GPUs. A batch size of 32 was the maximum size permissible by memory constraints for an input image of dimensions 290×384 pixels. Several measures were taken to avoid overfitting including a dropout layer after the first MaxPooling layer and 2 batch normalization layers. The batch normalization layers were placed after the convolutional layer and the first fully connected layer. Our model

was trained for 100 epochs, which amounted to a training time of 2 minutes, whereas a classification prediction for an unseen fingerprint image took less than a second per image. A schematic of the CNN architecture can be seen in Supplemental Figure 4 and model parameters in Supplemental Table 1.

Logistic regression and CNN modeling were repeated where clinically diagnosed and KS-like participants were excluded from the analysis because both groups may exhibit phenotypic differences compared with molecularly confirmed KS-diagnosed participants.

Results

Quality assurance and characteristics of the clinical cohort

A schematic summary of the study design can be seen in Figure 1A illustrating the study participants (n = 183, see Table 1 for group characteristics), the analysis of KS fingerprint pattern distinctiveness, and the 2 models (a logistic regression model and a CNN model) used to test the utility of fingerprints analysis for KS diagnosis. A total of 1830 fingerprint images were collected through the study, comprising 1080 images from the control group, 740 from the KS group, and 10 from the KS-like participant. A total of 61 out of 74 (82.4%) KS participants confidently reported that their pathological variant was found in a particular KS gene (either *KMT2D* or *KDM6A*), 5 (6.75%) reported a purely clinical diagnosis (although 1 of these had a variant of uncertain significance, *KMT2D* p.L449T), and 8 (10.8%) knew that a pathological genetic variant had been found in either *KMT2D* or *KDM6A* but were unsure which one and were thus grouped with the clinically diagnosed. A total of 30 out of 74 (40.5%) KS participants provided detailed molecular information, excluding 2 ambiguous results, regarding their genetic variant for *KMT2D* (see Figure 1B for variant location and translational impact) and *KDM6A* (see Figure 1C for variant location and translational impact). Combined molecular information can be seen in Supplemental Table 2. Detailed clinical information from the control group gathered after genetic counseling was available for 43 out of 108 (40%) participants and is summarized in Supplemental Table 3.

We used 3 different quality scores to assess fingerprint image quality: (1) inadequate collection; (2) Henry's pattern; and (3) the NFIQ2 score (see Supplemental Table 4). The fingerprint core was obscured or absent from the fingerprint pattern (excluding arch containing patterns) in 36 images (3.3%) of the control group cases, 119 images (17.7%) of the KS cases, and in 0 images for the KS-like participant. Image quality was inadequate for Henry's pattern categorization in 42 images (3.9%) of the control group cases, 133 images (17.3%) of the KS group, and 1 image (10%) of the KS-like participant. The NFIQ2 score for KS and KS-like cases combined into a single group had a median score of 8.50 with a range of [0, 71.0], and the control group had a median score of 40.0 with a range of [0, 88.0]. Supplemental Table 4 highlights the variation in quality scores across the different sampling locations, with the Baltimore collection site displaying the lowest scores. This discrepancy is attributed to suboptimal data collection, which was further supported by visual inspection.

Pattern characteristics of KS fingerprints—Single variable analysis

The FFR was seen in a total of 180 (16.7%) cases in the control group, 278 (37.6%) cases in the KS group, and 6 (60%) cases for the KS-like participant. Results of the preliminary analysis are summarized in Supplemental Table 5. At reevaluation, the mFFRC of the KS group was 14.0 (CI [12.9; 15.1]) and 18.3 (CI [16.6; 20.0]) for the control group (P = 6.3e−5). The KS-like participant had an mFFRC value of 13. The odds ratio for reevaluation of the preliminary variable of lack of individual pattern variability for the KS group compared with the control group was 3.8 (CI [1.43; 10.43], P = 3.4e−3) and for the simple pattern the odds ratio was 5.3 (CI [1.80; 16.45], P = 9.0e−4). The odds ratio for ulnar loops in KS compared with the control group was 1.6 (CI [1.26; 1.93], P = 2.0e−7) when reevaluated. The variable ridge density declined more in the control group than in the KS group (see Supplemental Figure 5). The only notable age-dependent differences in the mean density value can be seen in the age groups 20 to 29 (P = 8.8e−3) and 30 to 39 (P = .049).

A logistic regression model separates KS fingerprints from controls

The receiver operating characteristic curve for the logistic regression models can be seen in Figure 2A-F, in which the AUC for the primary model (Figure 2A), the verification model (Figure 2B), and the secondary model (Figure 2C) were 0.84 [0.75; 0.93], 0.78 [0.66; 0.90], and 0.82 [0.75; 0.89], respectively. The likelihood ratios for the 3 models were as follows: 24.0 at the threshold 0.72 for the primary model (Figure 2D); 4.6 at the threshold 0.73 for the validation model (Figure 2E); and 9.0 at the threshold 0.72 for the secondary model (Figure 2F). For the primary model and the validation model, the corresponding thresholds 0.72 and 0.73 had the highest likelihood ratio for each model; however, the highest likelihood ratio for the secondary model was at 0.80 in which the value was 12.0. Prevalence of secondary model guesses over the 0.72 threshold (KS positive) for KS subgroups were as follows: 17 of 39 (43.6%) for KS1, 1 of 7 (14.3%) for KS2, 4 of 12 (33.3%) for clinically diagnosed and 0 of 1 (0%) for KS-like, note the model sensitivity analysis was performed with LOOCV, which produces different sensitivity than if directly calculated from guess values over 0.72. The sensitivity and

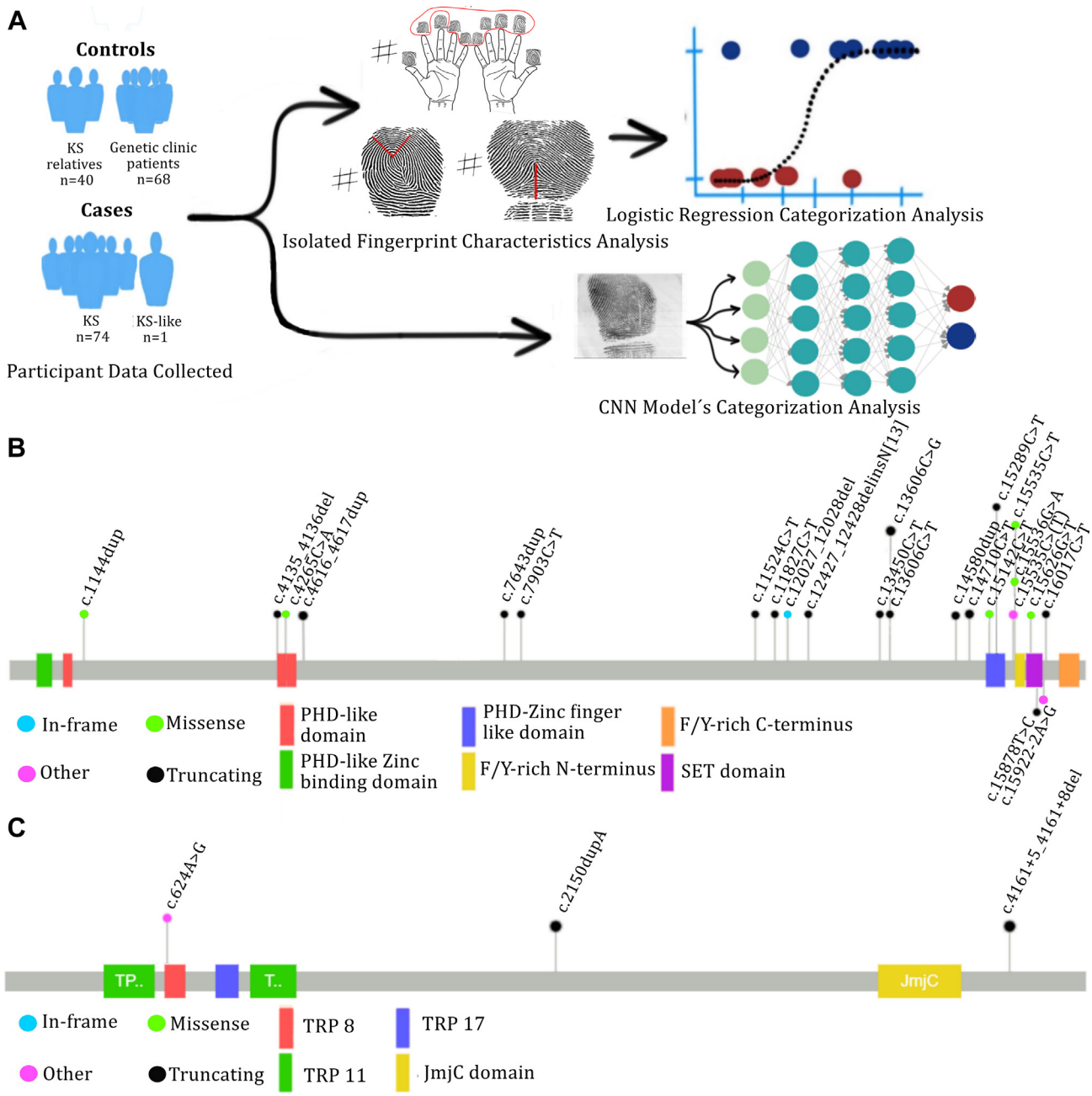

Figure 1 Schematic summary of the study design and information regarding molecular confirmation of participants. A. Data were collected from $n = 74$ KS participants, $n = 1$ KS-like participant and $n = 108$ controls. Fingerprint images from all participants were analyzed for differences in fingerprint characteristics. The analysis was used to explore classification ability of pre-determined fingerprint characteristics on individual participant bases by using logistic regression. Individual fingerprint images were also classified using a convolutional neural network (CNN) B. Collected participants genetic variants in the *KMT2D* gene. C. Collected participants genetic variants in the *KDM6A* gene. Large deletions ($n = 2$) were excluded from images (B) and (C).

specificity of the models can be seen graphically in Figure 3 (left) and their values in Supplemental Table 6.

A CNN model differentiates KS fingerprints from controls

Sensitivity and specificity of the CNN models trained with different data restrictions can be seen in Figure 3 (right) with values in Supplemental Table 7, both as 5-fold cross validation average and as results from held-out testing data. As expected, the model's performance improves when data of poor quality are removed from the data set, supporting our rationale of using quality measures to exclude images of poor quality. A slight decrease in specificity of the model occurs when trained on ridge enhanced images vs raw fingerprint images, when tested on held out test data

Table 1 Participant characteristics of the KS group, control group, and for the KS-like participant

	Control ($N = 108$)	Kabuki ($N = 74$)	Kabuki-like ($N = 1$)
Sex			
M	54 (50.0%)	31 (41.9%)	0 (0%)
F	54 (50.0%)	44 (58.1%)	1 (100%)
Ethnicity			
White	97 (89.8%)	55 (74.3%)	1 (100%)
Hispanic	3 (2.8%)	8 (10.8%)	0 (0%)
Black/African American	1 (0.9%)	4 (5.4%)	0 (0%)
Asian	4 (3.7%)	5 (6.8%)	0 (0%)
Other	3 (2.8%)	2 (2.7%)	0 (0%)
Age group [years]			
0-5	14 (13.0%)	11 (14.9%)	0 (0%)
6-12	22 (20.4%)	37 (50.0%)	1 (100%)
13-19	3 (2.8%)	11 (14.9%)	0 (0%)
20-29	16 (14.8%)	9 (12.2%)	0 (0%)
30-39	24 (22.2%)	4 (5.4%)	0 (0%)
40-49	20 (18.5%)	1 (1.4%)	0 (0%)
50-59	7 (6.5%)	1 (1.4%)	0 (0%)
≥60	2 (1.9%)	0 (0%)	0 (0%)
Kabuki gene			
KDM6A		8 (10.8%)	
KMT2D		53 (71.6%)	
Clinical		13 (17.6%)	
Genetic syndrome			
Confirmed	16 (14.8%)		
Suspected	18 (16.7%)		
KS relative	40 (37.0%)		
Unsuspected	34 (31.5%)		

Detailed clinical information accompanies the control group participants who enrolled from National University Hospital of Iceland, see Supplemental Table 3.

compared with the 5-fold cross validation. Prevalence of correct prediction of the CNN model sorted by the location where they were collected can be seen in Supplemental Tables 8 and 9. A notable difference can be seen in incorrectly categorized fingerprints from KS participants from Iceland and Seattle. The distribution of training data and testing data in relation to sampling location can be seen in Supplemental Table 10. For the CNN model in Supplemental Tables 8 and 9 the prevalence of correct prediction for the 5-fold cross validation was as follows: 210 of 320 (65.6%) for KS1, 40 of 56 (71.4%) for KS2, 74 of 96 (77.1%) for clinically diagnosed, and 0 of 6 (0%) for KS-like and for the held-out testing set was as follows: 22 of 31 (71.0%) for KS1, 2 of 4 (50%) for KS2, and 12 of 12 (100%) for clinically diagnosed.

Model performance with excluded clinically diagnosed and KS-like participants

The findings for logistic regression and CNN modeling, excluding clinically diagnosed and KS-like participants, are detailed in Supplemental Tables 11 and 12 and illustrated in Supplemental Figures 6 and 7. Secondary logistic regression at the threshold 0.64 resulted in a sensitivity of 39.13% [26.09%; 52.23%], specificity of 96.04% [92.08%; 99.0%], and positive likelihood ratio of 9.9. The CNN model resulted in a sensitivity of 44.23% and specificity of 94.12%, with a positive likelihood ratio of 7.52 when tested on unseen test data.

Discussion

In this study, we identified specific fingerprint characteristics that can effectively distinguish individuals with KS from the general population. We demonstrate 2 independent classification strategies, which could be used as a diagnostic aid for KS.

We observed 2 fingerprint characteristics that were significantly more common in the KS group: the mFFRC and the simple pattern. The lower mFFRC reported for KS individuals indicates a relatively smaller distance between the FFR and the fingerprint core compared with the control participants, which is suggestive of a different FFR mechanistic basis between the 2 groups. The ridge density distal to the core is either the same or increased in the KS group (Supplemental Figure 5), supporting the hypothesis of a separate etiology over the explanation that the ridge density is simply decreased. We believe that age differences do not account for the mFFRC differences because the fingerprint pattern itself remains constant from birth. This establishes mFFRC as an age-independent variable (although ridge density may be age dependent). The dual etiology of FFR could be explained by the following: first, as skin folding of the distal interphalangeal joint, appearing indiscriminatory of groups, and second, as skin folding of a compressed persistent fetal finger pad against a flat surface, specific to the KS group, causing the FFR to appear closer to the core. Notably, the mFFRC value for the KS-like participant (exhibiting persistent fetal finger pads) was 1 ridge lower than the average mFFRC value for KS, further supporting the folding hypothesis as one of FFR dual etiologies. An alternative explanation for a reduced mFFRC could stem from topographical and/or genetic abnormalities in individuals with KS, leading to the formation of the fingerprint core closer to the distal interphalangeal joint. In either scenario, the mFFRC can be attributed to an underlying syndromic process, whether it involves a direct genetic cause or a defect in volar pad regression. Another distinct feature of the KS group is increased homogeneity in fingerprint patterns presenting itself as 5.3 times higher odds of having a simple pattern. Increased pattern homogeneity may stem from homogenous finger pad development shaping early fetal pad topography and/or shared disruption in epigenetic control of limb maturing genes known to be associated with the development of fingerprint patterns.[6,7]

We demonstrate 2 methods capable of distinguishing individuals with KS from the general population (see

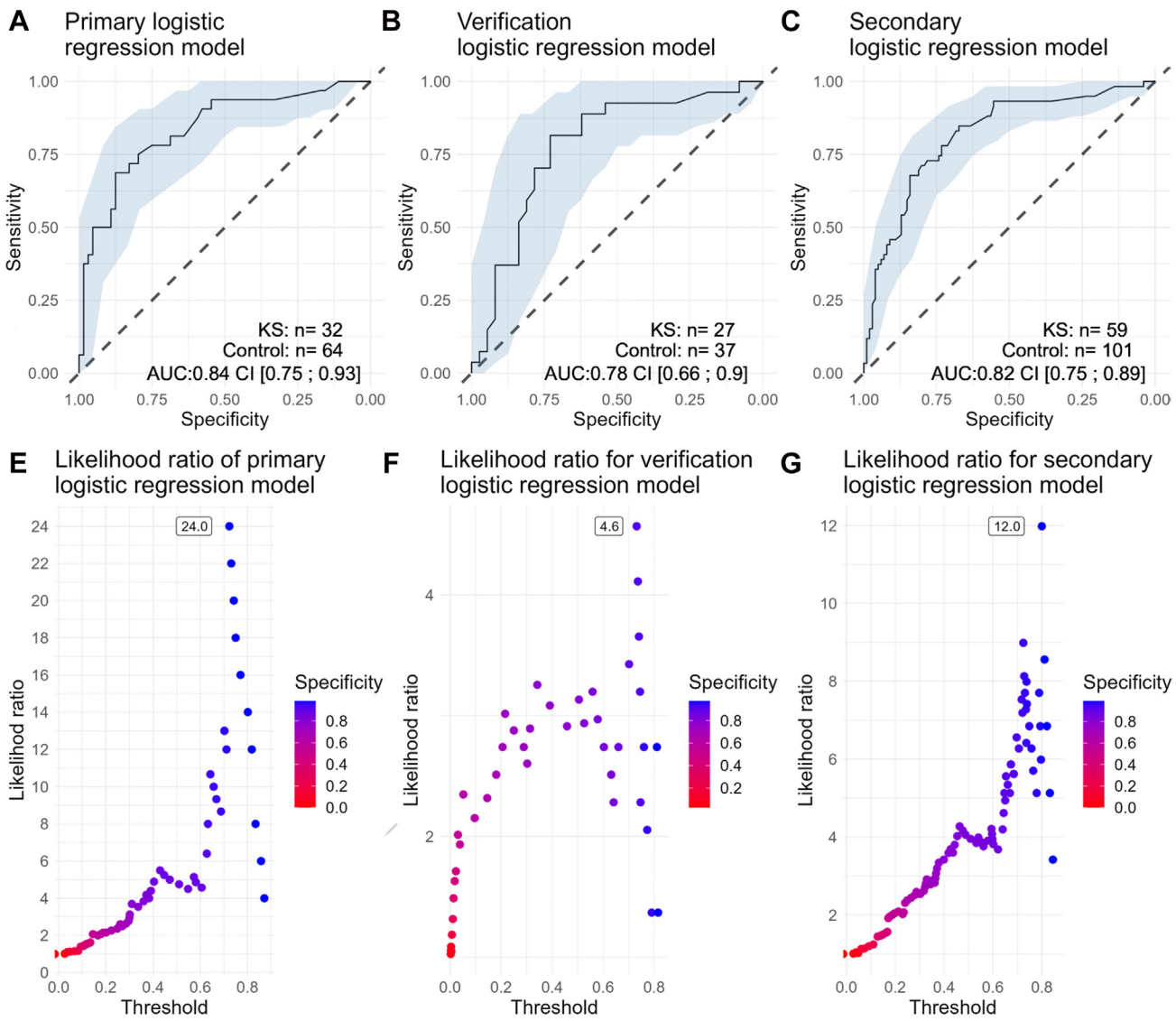

Figure 2 **Performance of logistic regression models.** A. ROC curve for the primary logistic regression model trained by $n = 32$ cases and $n = 64$ controls. B. ROC curve from the verification model where the primary model was tested on $n = 37$ controls and $n = 27$ cases of unseen participant data. C. ROC curve for the secondary logistic regression model in which data from (A) and (B) were combined, $n = 101$ controls and $n = 59$ cases. E-G. show the likelihood ratio of the model above each picture as a function of different thresholds, with corresponding specificity.

Figure 3 [left] or Supplemental Table 6 for the logistic regression model and Figure 3 [right] or Supplemental Table 7 for the CNN model). Regression models based on extracted fingerprint features achieved high specificity separation thresholds (over 90%), and the AUC values of the models were approximately 0.8 (Figure 2). The secondary model's threshold of 0.72 serves as an indicator of the diagnostic value of identified KS pattern characteristics because it was the most prominent threshold in the primary model and validated with unseen data (because of limited threshold outputs from the validation model the closest threshold to 0.72 was used, which was 0.73). The model exhibited a specificity of 96.04% (CI [92.08; 99.01]), sensitivity of 35.6% (CI [23.73; 47.46]), and a likelihood ratio of 9.0 (range: 3.00; 48.00). We also report highly promising results from using a CNN model based on individual fingerprint images. When tested on unseen data, the CNN model achieved a sensitivity of 76.6% and specificity of 91.2% with a likelihood ratio of 8.7, achieving higher sensitivity than the logistic regression model with superior clinical practicality by not relying on any fingerprint preassessment for pattern recognition (ie, no manual or semiautomatic pattern analysis was needed for processing). Furthermore, the CNN only needs 1 fingerprint image to evaluate a possible KS diagnosis. We note that using all 10 fingerprints for each individual instead of only using 1 image will likely increase the accuracy of the CNN method. However, this approach requires substantially more training data, which we aim to pursue in our future studies. Although CNNs are often considered black box methods because of

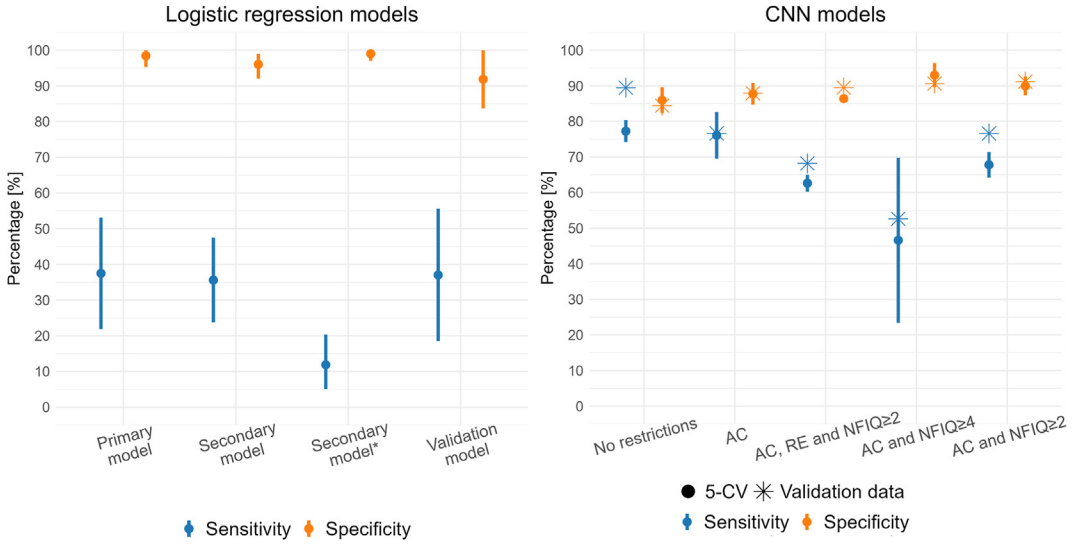

Figure 3 **Sensitivity and specificity comparison.** The circles represent the point estimates of sensitivity and specificity for the logistic regression models (left) and 5-fold cross validation (5-CV) CNN model (right). The vertical lines represent the 95% confidence intervals (CI) of the point estimates. The 8-pointed star represents the sensitivity and specificity when CNN model (right) was tested on unseen (held-out) test data. The logistic regression models use the same thresholds as in Supplemental Table 6 in which the secondary model* uses threshold 0.80. Adequate collection (AC) includes data in which collection error did not result in the absence of the fingerprint core (excluding arch type patterns). NFIQ2 is short for the NFIQ2 scoring system and RE stands for ridge enhancement.

their unknown classification traits, the increase in specificity resulting from excluding suboptimal quality data supports the notion that the CNN model utilizes KS-specific fingerprint characteristics for classification, see Supplemental Figure 7 (right) or Supplemental Table 7. This aligns with the greater informational variance toward the core of the fingerprint patterns compared with their periphery. Although ridge enhancement produced slightly inferior results compared with unenhanced images, it might produce better results in practice by decreasing interindividual sampling error.

The high specificity of 91% to 96% for both the logistic regression and CNN models, along with a likelihood ratio of 8.7 to 9.0, can greatly benefit the clinical diagnosis of KS. The practicality of using this diagnostic aid lies in supporting KS suspicion, either for targeted genetic testing when the clinical suspicion is low, reducing costs and time to diagnosis, or for supporting clinical diagnosis when the suspicion is high and genetic testing is unavailable. For proof of clinical utility, further research will be needed to show that KS can be distinguished from a more relevant control group. This can be done by directly testing the model diagnostic accuracy on an unseen KS group with a control group consisting of participants with developmental delay, facial dysmorphic features, and intellectual disability of known etiology unrelated to KS.

As can be seen in Supplemental Tables 11 and 12, as well as in Supplemental Figures 6 and 7, the repeated analysis, in which the KS-like and clinically diagnosed participants were excluded, produces comparable results to the primary analysis. The likelihood ratio was similar in the logistic regression analysis with a shift in thresholds' values, see Supplemental Tables 6 and 11 for value comparison. The trend of decreased sensitivity with an increase in specificity could also be seen in the CNN model, see Supplemental Figure 7 (right), although markedly lower sensitivity and increased specificity could be seen with more stringent quality restrictions. Decreased sensitivity could be explained by decreased data points for CNN pattern learning. The increased specificity, although small, could be explained by increased phenotype variance of the excluded group or by excluding a few misdiagnosed KS cases. Hence, fewer but more specific patterns were extracted with the CNN. With an increased data set, KS subgroup analysis could be performed to assess if there are marked dermatoglyphic differences between KS1, KS2, clinically diagnosed, and KS-like participants. One would not expect much of a difference if the dermatoglyphic changes are only reliant on abnormal volar pad regression.

Although efforts were made to standardize the collection method and remove inadequate data, there is a potential risk of collection bias resulting in artificially higher FFR prevalence in the KS group, given that multiple individuals collected the fingerprint samples. However, nearly all collectors obtained samples from both KS and control participants. Inadequate data were mainly concentrated among a few participants in which Henry's classification was impossible, leading to the removal of most of their fingerprints from the analysis. The CNN analysis might be more sensitive to collection bias because it is directly reliant on fingerprint images. Although notable differences in correct CNN model classification were observed based on the collection location, they were not significant enough to raise concerns about location-based bias in the model

classification (see Supplemental Tables 8 and 9). A limited number of participants in location-specific subgroups may explain the difference. Data were distributed equally between training and testing in relation to location (see Supplemental Table 10). Finally, the relatively small data set used for training the CNN, compared with other DNN studies, could limit the diagnostic power of our model and potentially, increase the likelihood of unrelated characteristics explaining the CNN model's classification capability. Future work includes investigating the possibility of enhancing the model's classification performance by utilizing a larger and more balanced training data set.

The age range 0 to 5 is wide for this specific age group and was skewed toward 4-to-5-year olds for the KS group. This is caused by the difficulty of recruiting infants and toddlers to the study, both because this is a more vulnerable age and because of the decreased likelihood of having a diagnosis at such an early age. In the KS group, 1 infant and 1 toddler were included, whereas the control group included 1 infant and 9 toddlers. Because fingerprint patterns are stable from birth, it opens the possibility of extrapolation of our results to infants and toddlers in the absence of data from that age group, which we will confirm with future research.

Molecular information was missing for a subset of KS participants, despite the vast majority having an official diagnosis made by a clinical geneticist. The majority were able to clearly report which gene was affected. However, the collection of specific molecular details was often hindered by the settings from which the data were collected, primarily at patient conferences, thereby limiting the extent of information that could be obtained (see Supplemental Table 2). The 17.6% of KS cases of this study categorized as clinically diagnosed, including those unable to report genetic diagnosis with certainty, was similar to the reported clinical diagnosis rate of 14.2% observed among 1369 KS individuals.[33] Higher prevalence could be attributed to partial misclassification of individuals that could not specify genetic diagnosis in either *KMT2D* or *KDM6A*.

Although a subset of the control group had suspected genetic disorders (see Supplemental Table 3) the characteristics of the control group as whole are nonspecific and largely unrelated to the differential diagnosis of KS. Occurence of persistent fetal fingertip pads was not documented during the collection of fingerprints, making it challenging to ascertain whether our findings are specific to the genetic disruption associated with KS or whether they are contingent on the presence of persistent fetal fingertip pads. Further work is needed to assess if our findings can reliably distinguish KS fingerprint from other syndromes that feature persistent fetal fingertip pads. If our findings are contingent on persistent fetal fingertips pad or the underlying cause of their disrupted regression in utero, it opens up the possibility of distinguishing numerous rare syndromes characterized by persistent fetal fingertip pads from the general population through fingerprint analysis. The KS-like participant, who exhibited prominent fetal fingertip pads, was distinguishable from KS cases, as negative results in relation to KS diagnosis were obtained from both the CNN model and logistic regression. We can draw limited conclusions from this single KS-like participant, but it suggests that our findings are not solely dependent on mFFRC. In future work, conducting a targeted expansion of related Mendelian disorders of the epigenetic machinery[34] would also be valuable for the assessment of KS fingerprint pattern distinctiveness because the wide-ranging symptomatic effects of epigenetic disruption might produce similar dermatoglyphic abnormalities.

Previous work has focused on differentiating between KS1 and KS2 rather than from clinically similar individuals with alternative diagnoses.[35,36] There is 1 facial based image CNN model that differentiates KS from healthy control group, which reported a sensitivity of 91% and a specificity of 100% when tested on unseen test data of $n = 11$ KS and $n = 13$ control participants.[36] The model's performance in clinical settings was therefore uncertain as is with our method. One advantage of our method is that fingerprints are stable from birth, but facial dysmorphic features are age dependent. It would be interesting to assess if combined facial image-based CNN and fingerprint-based CNN would complement each other in clinical settings and if fingerprint-based CNN could potentially be more beneficial in infants.

In this study, fingerprint data were collected through a smartphone connected to an external fingerprint scanner. Future advancements may enable strategies using smartphone cameras or built-in scanners (Gupta S, Anand S, Rai A. Fingerprint Extraction Using Smartphone Camera. Published Online August 2, 2017. https://doi.org/10.48550/arXiv.1708.00884),[37] eliminating the need for an external device. Such an approach could democratize KS diagnosis in diverse populations, addressing global disparities in genetic services access. This especially applies to regions with limited genetic testing resources, such as developing countries, rural areas, and remote locations.[10,11,38] However, fingerprint scanners serve as an affordable and easily accessible alternative (cost per scanner used: $72), positively affecting the cost-benefit ratio for medical clinics.

The key conclusion of our research is the success of 2 independent approaches in classifying KS from control using fingerprints alone, suggesting utility for smartphones as a diagnostic aid for genetic diseases in the near future. Future focus will be on assessing clinical utility of the discovered methods by comparing KS fingerprints to clinically similar participants along with combining clinical KS features, such as palpebral fissure or intellectual disability (IQ < 70), for improved sensitivity.

Data Availability

The original data set supporting the current study has not been deposited in a public repository because of pending

patent application and sensitivity of the data set, but the original data set is available from the corresponding author by reasonable request.

Acknowledgments

The authors thank the families and participants who took part in the project. The authors thank the KabukiUK charity, the staff of the Genetic counseling department of Landspitali University Hospital, and Kabuki Syndrome Foundation for their collaboration with participant recruitment. The authors thank the staff at the Department of Genetics and Molecular Medicine at Landspitali, as well as Amanda Gamboa (KSF), Jacqueline Harris (JHH), and Allison Kalinousky (JHH) for their assistance in fingerprint collection.

Funding

H.T.B., V.I.A., and P.A.B. were funded by a grant from the Louma G. Foundation. V.I.A. and A.F. were funded by grants from the Icelandic Student Innovation fund.

Author Contributions

Conceptualization: H.T.B., L.M.E.; Data Curation: V.I.A.; Formal Analysis: V.I.A.; Methodology: V.I.A.; Investigation: V.I.A.; Funding Acquisition: H.T.B., L.M.E.; Visualization: V.I.A.; Writing-original draft: H.T.B., L.M.E., V.I.A.; Writing-review and editing: H.T.B., L.M.E., P.A.B., V.I.A., A.F.; Software Development (CNN model): P.A.B.; Software Development (GenePrint app): A.F.

Ethics Declaration

Informed consent for individuals with KS and family members was obtained for all 108 control and 75 cases using IRB approved protocols from either the Johns Hopkins Hospital (NA_00079185) or from the ethical board of Landspitali University Hospital (VRN_211118) and the National Bioethics Committee of Iceland (VSN_21-228). The data were de-identified after data collection

Conflict of Interest

The authors would like to declare that they have no actual or potential competing interests other than a subset of authors (Hans Tomas Bjornsson, Lotta Maria Ellingsen, and Viktor Ingi Agustsson) having filed a patent application for the diagnosis of rare diseases using fingerprint analysis, based on the findings presented in the current manuscript (filing date 18/12/23). Dr Bjornsson is a consultant for Mahzi therapeutics and founder for Kaldur Therapeutics.

Declaration of AI and AI-Assisted Technologies in the Writing Process

During the preparation of this work, the authors used ChatGPT-3.5 to improve readability of the manuscript. After using this tool/service, the authors reviewed and edited the content as needed and take full responsibility for the content of the publication.

Additional Information

The online version of this article (https://doi.org/10.1016/j.gimo.2024.101884) contains supplemental material, which is available to authorized users.

References

1. Cummins H, Talley C, Platou RV. Palmar dermatoglyphics in mongolism. *Pediatrics*. 1950;5(2):241-248. http://doi.org/10.1542/peds.5.2.241
2. Verbov J. Clinical significance and genetics of epidermal ridges-A review of dermatoglyphics. *J Invest Dermatol*. 1970;54(4):261-271. http://doi.org/10.1111/1523-1747.ep12258550
3. Suzumori K. Dermatoglyphic analysis of fetuses with chromosomal abnormalities. *Am J Hum Genet*. 1980;32(6):859-868.
4. Reed T, Opitz JM. Dermatoglyphics in medicine—problems and use in suspected chromosome abnormalities. *Am J Med Genet*. 1981;8(4):411-429. http://doi.org/10.1002/ajmg.1320080407
5. Machado JF, Fernandes PR, Roquetti RW, Filho JF. Digital dermatoglyphic heritability differences as evidenced by a female twin study. *Twin Res Hum Genet*. 2010;13(5):482-489. http://doi.org/10.1375/twin.13.5.482
6. Li J, Glover JD, Zhang H, et al. Limb development genes underlie variation in human fingerprint patterns. *Cell*. 2022;185(1):95-112.e18. http://doi.org/10.1016/j.cell.2021.12.008
7. Kücken M, Newell AC. Fingerprint formation. *J Theor Biol*. 2005;235(1):71-83. http://doi.org/10.1016/j.jtbi.2004.12.020
8. Seidenberg-Kajabova H, Pospisilova V, Vranakova V, Varga I. An original histological method for studying the volar skin of the fetal hands and feet. *Biomed Pap Med Fac Univ Palacky Olomouc Czech Repub*. 2010;154(3):211-218. http://doi.org/10.5507/bp.2010.032
9. Muigai AWT. Expanding global access to genetic therapies. *Nat Biotechnol*. 2022;40(1):20-21. http://doi.org/10.1038/s41587-021-01191-0
10. Cornetta K, Bonamino M, Mahlangu J, Mingozzi F, Rangarajan S, Rao J. Gene therapy access: global challenges, opportunities, and views from Brazil, South Africa, and India. *Mol Ther*. 2022;30(6):2122-2129. http://doi.org/10.1016/j.ymthe.2022.04.002
11. Thong MK, See-Toh Y, Hassan J, Ali J. Medical genetics in developing countries in the Asia-Pacific region: challenges and opportunities. *Genet Med*. 2018;20(10):1114-1121. http://doi.org/10.1038/s41436-018-0135-0
12. Gurovich Y, Hanani Y, Bar O, et al. Identifying facial phenotypes of genetic disorders using deep learning. *Nat Med*. 2019;25(1):60-64. http://doi.org/10.1038/s41591-018-0279-0
13. Adam MP, Banka S, Bjornsson HT, et al. Kabuki syndrome: international consensus diagnostic criteria. *J Med Genet*. 2019;56(2):89-95. http://doi.org/10.1136/jmedgenet-2018-105625

14. Niikawa N, Kuroki Y, Kajii T. The dermatoglyphic pattern of the Kabuki make-up syndrome. *Clin Genet*. 1982;21(5):315-320. http://doi.org/10.1111/j.1399-0004.1982.tb01378.x
15. Niikawa N, Kuroki Y, Kajii T, et al. Kabuki make-up (Niikawa-Kuroki) syndrome: a study of 62 patients. *Am J Med Genet*. 1988;31(3):565-589. http://doi.org/10.1002/ajmg.1320310312
16. Zhang L, Pilarowski G, Pich EM, et al. Inhibition of KDM1A activity restores adult neurogenesis and improves hippocampal memory in a mouse model of Kabuki syndrome. *Mol Ther Methods Clin Dev*. 2021;20:779-791. http://doi.org/10.1016/j.omtm.2021.02.011
17. Benjamin JS, Pilarowski GO, Carosso GA, et al. A ketogenic diet rescues hippocampal memory defects in a mouse model of Kabuki syndrome. *Proc Natl Acad Sci U S A*. 2017;114(1):125-130. http://doi.org/10.1073/pnas.1611431114
18. Bjornsson HT, Benjamin JS, Zhang L, et al. Histone deacetylase inhibition rescues structural and functional brain deficits in a mouse model of Kabuki syndrome. *Sci Transl Med*. 2014;6(256):256ra135-256ra135. https://doi.org/10.1126/scitranslmed.3009278.
19. Rajpurkar P, Chen E, Banerjee O, Topol EJ. AI in health and medicine. *Nat Med*. 2022;28(1):31-38. http://doi.org/10.1038/s41591-021-01614-0
20. Senior AW, Evans R, Jumper J, et al. Improved protein structure prediction using potentials from deep learning. *Nature*. 2020;577(7792):706-710. http://doi.org/10.1038/s41586-019-1923-7
21. Cheng J, Novati G, Pan J, et al. Accurate proteome-wide missense variant effect prediction with AlphaMissense. *Science*. 2023;381(6664):eadg7492. http://doi.org/10.1126/science.adg7492
22. Marwaha A, Chitayat D, Meyn MS, Mendoza-Londono R, Chad L. The point-of-care use of a facial phenotyping tool in the genetics clinic: enhancing diagnosis and education with machine learning. *Am J Med Genet A*. 2021;185(4):1151-1158. http://doi.org/10.1002/ajmg.a.62092
23. Reguant R, Brunak S, Saha S. Understanding inherent image features in CNN-based assessment of diabetic retinopathy. *Sci Rep*. 2021;11(1):9704. http://doi.org/10.1038/s41598-021-89225-0
24. Yadav SS, Jadhav SM. Deep convolutional neural network based medical image classification for disease diagnosis. *J Big Data*. 2019;6(1):113. http://doi.org/10.1186/s40537-019-0276-2
25. Dildar M, Akram S, Irfan M, et al. Skin cancer detection: a review using deep learning techniques. *Int J Environ Res Public Health*. 2021;18(10):5479. http://doi.org/10.3390/ijerph18105479
26. Atlason HE, Love A, Robertsson V, et al. A joint ventricle and WMH segmentation from MRI for evaluation of healthy and pathological changes in the aging brain. *PLoS One*. 2022;17(9):e0274212. http://doi.org/10.1371/journal.pone.0274212
27. Deshmukh U. Fingerprint-enhancement-Python. GitHub. Accessed April 4, 2022. https://github.com/Utkarsh-Deshmukh/Fingerprint-Enhancement-Python
28. Tabassi E, Fiumara G. NFIQ. Accessed December 26, 2022. https://www.nist.gov/services-resources/software/nfiq-2
29. Yager N, Amin A. Fingerprint classification: a review. *Pattern Anal Appl*. 2004;7(1):77-93. http://doi.org/10.1007/s10044-004-0204-7
30. Skeletonization-by-Zhang-Suen-Thinning-Algorithm/thinning. py at master · linbojin/Skeletonization-by-Zhang-Suen-Thinning-Algorithm. GitHub. Accessed April 4, 2022. https://github.com/linbojin/Skeletonization-by-Zhang-Suen-Thinning-Algorithm
31. Robin X, Turck N, Hainard A, et al. pROC: an open-source package for R and S+ to analyze and compare ROC curves. *BMC Bioinformatics*. 2011;12(1):77. http://doi.org/10.1186/1471-2105-12-77
32. Kuhn M, Wing J, Weston S, et al. caret: classification and regression training. CRAN. Accessed January 8, 2023. https://CRAN.R-project.org/package=caret
33. Barry KK, Tsaparlis M, Hoffman D, et al. From genotype to phenotype-a review of Kabuki syndrome. *Genes*. 2022;13(10):1761. http://doi.org/10.3390/genes13101761
34. Bjornsson HT. The Mendelian disorders of the epigenetic machinery. *Genome Res*. 2015;25(10):1473-1481. http://doi.org/10.1101/gr.190629.115
35. Rouxel F, Yauy K, Boursier G, et al. Using deep-neural-network-driven facial recognition to identify distinct Kabuki syndrome 1 and 2 gestalt. *Eur J Hum Genet*. 2022;30(6):682-686. http://doi.org/10.1038/s41431-021-00994-8
36. Hennocq Q, Willems M, Amiel J, et al. Next generation phenotyping for diagnosis and phenotype–genotype correlations in Kabuki syndrome. *Sci Rep*. 2024;14(1):2330. http://doi.org/10.1038/s41598-024-52691-3
37. Gottschlich C, Huckemann S. Separating the real from the synthetic: minutiae histograms as fingerprints of fingerprints. *IET Biom*. 2014;3(4):291-301. http://doi.org/10.1049/iet-bmt.2013.0065
38. Hawkins AK, Hayden MR. A grand challenge: providing benefits of clinical genetics to those in need. *Genet Med*. 2011;13(3):197-200. http://doi.org/10.1097/GIM.0b013e31820c056e